Bulletin of Earth Sciences of Thailand

OVERPRESSURE IDENTIFICATION USING SEISMIC AND WELL LOGS, PATTANI BASIN, GULF OF THAILAND

Yonradee Sutjarittanan*

Department of Geology, Faculty of Science, Chulalongkorn University, Bangkok, 10330, Thailand
*Corresponding author email: kul_narak69@hotmail.com

Abstract

The prevention of drilling kicks, the drilling risk in connection with expected formation pressure and the casing design are typical industry problems associated with pore pressure prediction before and during exploration well drilling. Currently, seismic velocities still remain a major input for pre-drill prediction. This is especially true for frontier depth intervals within the explored areas. The main topic in this thesis is overpressure. The overpressure zone is the zone that the pressure exceeds normal hydrostatic pressure at a given depth. This thesis focuses on two fields in Southern Pattani Basin which are Funan and South Gomin fields. Funan field has high pressure whereas South Gomin has lower pressure compared to Funan field. Seismic velocity contains information about lithology changes including velocity in each rock layer. An extraction of the target overpressure signal from seismic velocity input is based on theoretical prediction which is then compared to the observed relevant seismic velocity information to detect changes related an overpressure anomaly. The seismic velocity data from pre-stack time migration (PSTM) velocity cube can be converted to interval velocity by Dix's equation and used for investigating possible overpressure anomalies. The overpressure zone shows slower interval velocity compared to hydrostatic pressure zone. The slower interval velocity can be visualized in some areas by velocity isochronal mapping and volume changes. Also, Eaton's method was tested to predicted pore pressure from seismic volume. The result of pressure prediction using seismic velocities is restricted by the resolution of seismic velocity picking and cause of overpressure.

Keywords: Overpressure, Hydrostatic pressure, PSTM velocity, Seismic velocity, Interval velocity, Isochronal velocity mapping

1. Introduction

Pore pressure prediction before and during exploration well drilling is important to prevent drilling mud losses or kicks due to unexpected formation pressures. It is also important for determining optimal casing design. Currently, seismic velocities, if proven predictive for overpressure identification, remain a major input for pre-drill prediction. This is especially true for frontier depth intervals within the explored areas.

The target phenomenon in this thesis is the overpressure zone which is the zone that the pressure exceeds normal hydrostatic pressure at a given depth. There are two previous studies using well data to predict pore pressure in Moragot Field (Bunyanupong, 2014 and Amonpantang, 2010). Those two studies have proven successful post-drilled method using well logs data following Eaton's method (Eaton, 1975). Furthermore, another study identifying seismic characteristics related to overpressure in Moragot and Pailin fields was completed using seismic velocity changes for pre-drilled prediction (Kananithikorn, 2015). Therefore, the main objective of this thesis is to identify seismic characteristics and analyze well log data related to overpressure in Funan and South Gomin fields for pre-drilled prediction. Seismic velocity and well logs are the main data used in this study.

2. General Geology of the study area

The Gulf of Thailand lies in the middle of a series of Tertiary rift basins that run northwards into onshore northern Thailand and southeastwards offshore Thailand. The Pattani Basin is approximately 270 x 100 km (Watcharanantakul and Morley, 2000). The Basin morphology is controlled by a series of major en-echelon listric faults that bound half grabens in a linear belt running the length of the trough (Kornsawan, 1999). It is thought to be the result of oblique-slip extensional rifting and East to West (E-W) extension during the Eocene rifting event (personal communication - Chevron Offshore Thailand Ltd., 2001). The structural configuration in the syn-rift period had a significant influence on deposition in the Gulf of Thailand. Faults are activated through time while the deposition of sediments, which are eroded from the structural high provenance, is continuous. The syn-rift section, Oligocene to Early Miocene age, displays a series of major en-echelon extensional faults which control the basin morphology as a half-graben and graben-type basin (Morley, 2004).

Overburden of sediment and hydrocarbon generation are considered to be the major mechanisms for generating overpressure in the sandstone reservoirs in Gulf of Thailand. Source rock studies (Rui Lin, 2006) indicate that the thermally mature zone occurs approximately at the depth of 6,000 ft and it is unlikely that any significant amounts of hydrocarbons were generated prior to the maturation depth (Figure 1). This study area covers two fields in two subbasins; Funan and South Gomin fields are separated by bounding faults located in the

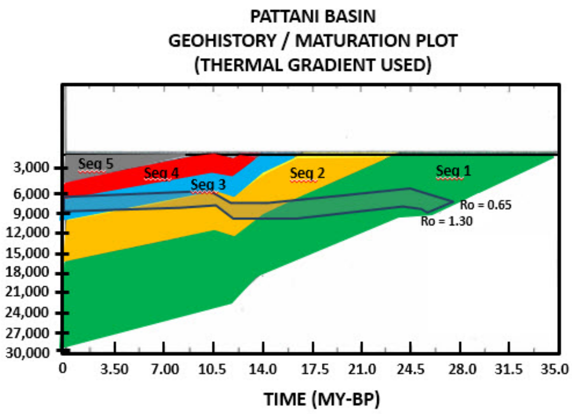

Figure 1 This diagram indicates that hydrocarbon generation window starts from 6,000 ft (approx.2,000m) to 9,000ft (approx.3,000m) (thermal gradient used) in Pattani Basin (modified from Burial history diagram and maturation window from internal report; Chevron Texaco (Offshore) Thailand Ltd., 2001)

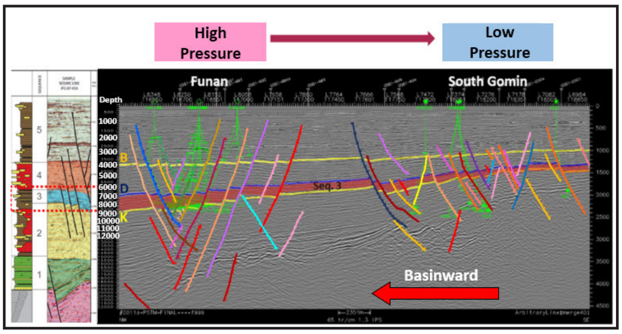

Figure 2 This diagram illustrates the structural style and stratigraphic units in the study area (Modified from Chevron Texaco (Offshore) Thailand Ltd., 2001). The basin morphology is controlled by a series of major faults that bound two half grabens (Funan and South Gomin) separated from each other. The interested window is Sequence 3 shaded as red color.

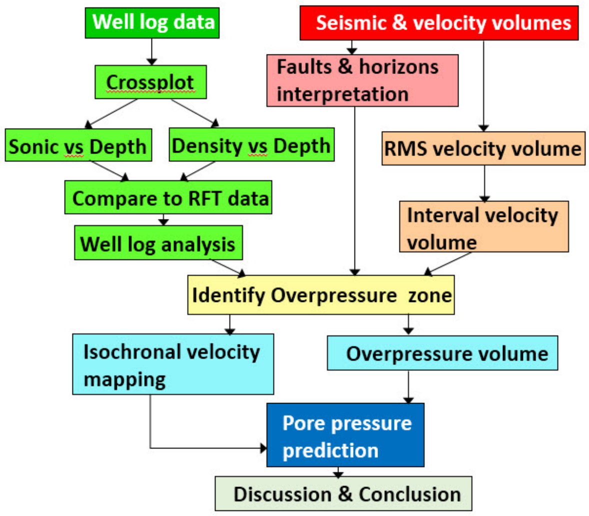

southern part of the Pattani Basin, Gulf of Thailand (Figure 2). The fault system in these two areas is a normal fault system with both west- and east-dipping faults forming half-graben structures.

4. Result and Interpretation

4.1) Overpressure observed from well log

In normal compaction situation, the formation's velocity and bulk density increase with depth. In overpressure, both velocity and density tend to be lower than normal pressure because seismic velocity is a function of the density and strength modulus of the rocks through which the energy passes; therefore,both density and strength are affected by abnormal pore pressure. Increasing pore pressure softens the rock elastic bulk modulus by lowering density and velocities. The resulting seismic profiles show unusually slow interval velocity and indicate an overpressured interval.

Sonic and density values of sand, silt and shale were plotted with depth as shown in Figure 3 (crossplot row A) and Figure 4 (crossplot row C) respectively. However, the sonic plot and density plot versus depth of shale show the trends clearer than sand and silt. This might be because the measurements in sands are affected from various types of fluid enclosed in rock porosity whereas shale trends are more likely to correlate with overpressure effect.

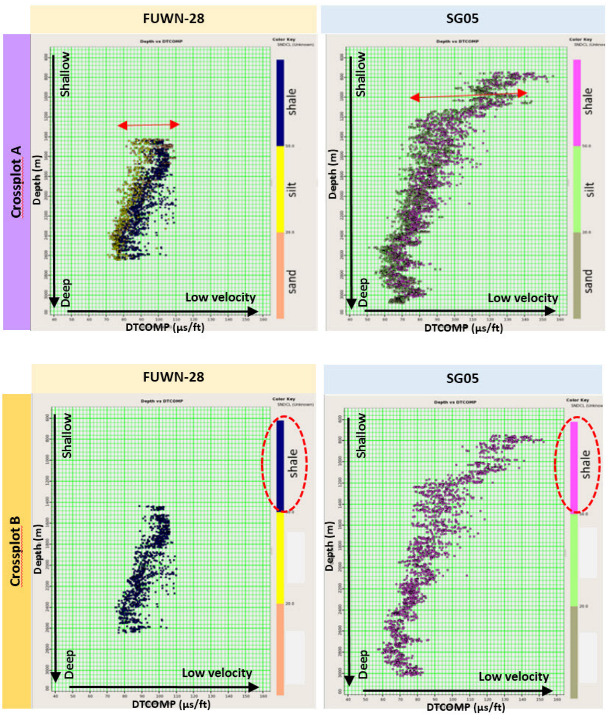

Figure 3 Crossplots in row A are the plots of sonic values of sand, silt and shale plotted between depth (y-axis) and sonic values (x-axis). Crossplots in row B are the plots of sonic values of shale (only) plotted between depth (y-axis) and sonic values (x-axis). The data points from sand, silt and shale (crossplots in row A) are quite sparse and they are not aligned as a trend compared to data points from shale only (crossplots in row B).

Therefore, in this study, the main plots are the sonic values and density values of shale plotted versus depth shown in Figure 3 (crossplot row B) and Figure 4 (crossplot row D) respectively. From the sonic plot and density plot, at the same depth interval, sonic values from well SG05 (hydrostatic well) have faster velocity in sonic plot and denser values in density plot than well FUWN-28 (overpressure well). Since SG07 has a shallower TD than SG05 and the data points are not enough to compare in overpressure zone therefore SG05 will be used to represent the normal pressured well. The density and sonic data from FUWN-28 and SG05 are plotted and shown in Figure 3, 4 and 5.

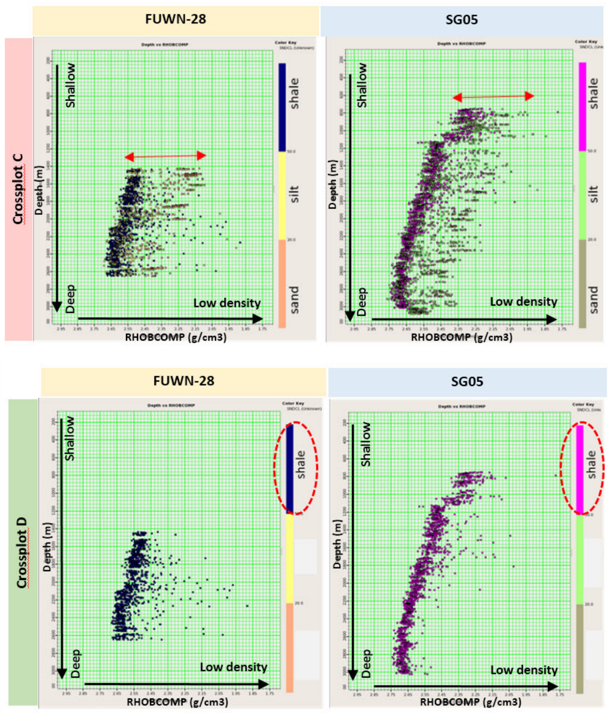

Figure 4 Crossplots in row C are the plots of density values of sand, silt and shale plotted between depth (y-axis) and density (x-axis). Crossplots in row D are the plots of density values of shale (only) plotted between depth (y-axis) and density (x-axis). The data points from sand, silt and shale (crossplots in row C) are quite sparse and they are not aligned as a trend compared to data points from shale only (crossplots in row D).

4.2) Overpressure observed on well-tie-to-seismic

Seismic responds differently in the subsurface depending on rock properties in each layer. Acoustic impedance is the product of density and seismic velocity, which varies among rock layers. The difference in acoustic impedance between rock layers affects the reflection coefficient which is the ratio of amplitude

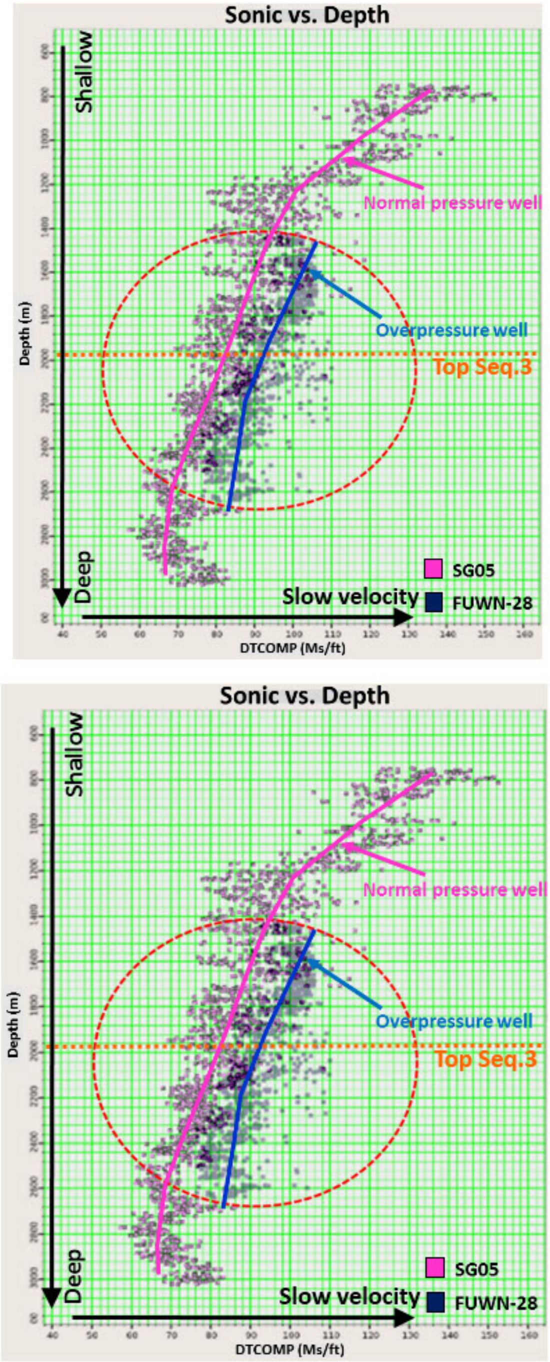

Figure 5 From crossplot at the top, at the same depth, the sonic data from SG05 colored in purple (normal pressure well) shows less slowness (faster in velocity) than FUWN-28 colored in dark blue (overpressure well) which it supports the fact that overpressured zones have a slower velocity (because of abnormally high porosity and pressure) than normal shales at a given depth. From crossplot below, at the same depth, the density data from SG05 (normal pressure well) is denser than density data from FUWN-28 (overpressure well) which it supports the fact that undercompacted shales, characteristic of overpressured zones, have a lower density than normal shales at a given depth.

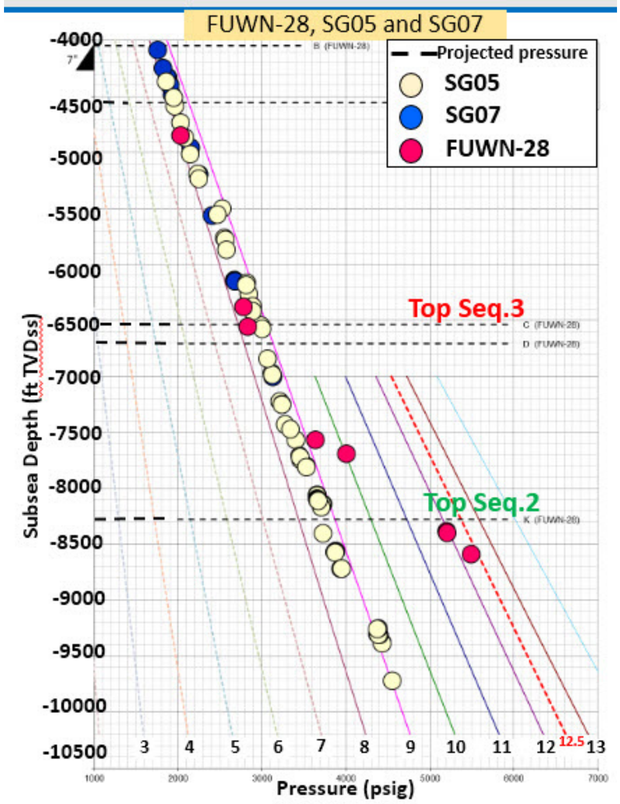

Figure 6 The profile illustrates that SG07 remains hydrostatic pressure except at well TD which pressure increases slightly up to 8.6 ppg. For SG05, the pressure starts increasing slightly at around C marker (Top of Sequence 3) and continue rising up to 8.8 ppg at well TD. However, FUWN-28 shows that the pressure start rising over hydrostatic pressure around C marker (Top of Sequence 3) and the highest pressure recorded is 12.3 ppg at well TD. It can be observed that overpressure from FUWN-28 starts from C marker which is related to the top of Sequence 3; however, SG05 and SG07 do not show overpressure increasing at C marker.

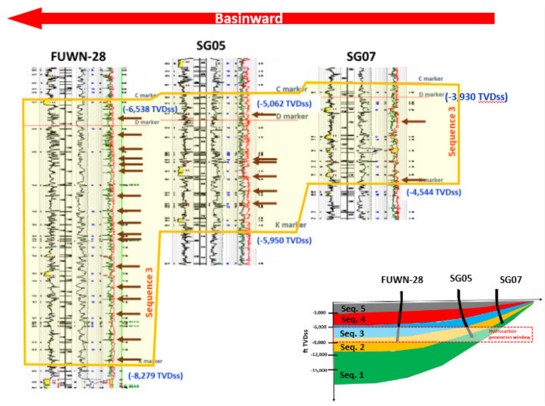

Figure 7 FUWN-28, SG05 and SG07 were ordered respectively from west to east (or from basin center to basin flank). Therefore, Sequence 3 in FUWN-28, which is located into the direction of basin center, is thicker than SG05 and SG07 which is located at the basin flank.

These well logs also show that Sequence 3 in each well has higher organic shale content than sequence above and below it. Also, Sequence 3 in FUWN-28 has higher portion of organic rich shale (shown in brown arrows) than Sequence 3 in SG05 and SG07 wells.

of the reflected wave to the incident wave or how much energy is reflected. In order to relate well data to seismic data, well-tie-to-seismic is the main process to perform. Well-seismic ties allow well data, measured in units of depth, to be compared to seismic data, measured in units of time. This allows us to relate horizon identified in a well with specific reflections on the seismic section. In this study, synthetic seismograms were generated from both sonic and density logs. The synthetic trace is compared to the real seismic data collected near the well location. The synthetic seismograms show good correlation.

Furthermore, velocity function plot (time-depth conversion plot) from these 3 wells (FUWN-28, SG05 and SG07) shows 2 different velocity trends which are fast velocity trend and slow velocity trend corresponding to the pressure in wells as shown in the Figure 8. The fastest velocity trend is observed in well SG05 and SG07, which is normal pressure well; whereas, overpressure well (FUWN-28) shows slower velocity trend. The result from this velocity plot supports the fact that overpressure zones can be identified as a slower velocity zone.

From figure 8, the velocity function of FUWN-28 (overpressure well) is the slowest which is slower than velocity function of SG05 and SG07. Seismic velocity is a function of the density and strength modulus of the rock through which the energy passes. Both density and strength are affected by abnormal pore pressure. Anomalously high pore pressure zones are often associated with high porosities and low seismic velocities. Thus, the result from this velocity plot supports the fact that overpressure zones can be identified as a slower velocity zone.

4.3) Overpressure observed on seismic data

Overpressure zones can be detected as slower interval velocity zones in the seismic velocity volume. Consequently, the seismic

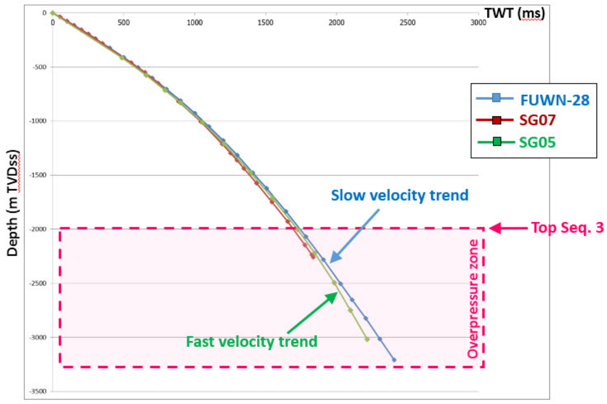

Figure 8 Velocity plot from well-tie-to-seismic for 3 wells; FUWN-28 (overpressure well), SG05 and SG07 (normal pressure well). The velocity function plot from these 3 wells (FUWN-28, SG05 and SG07) shows 2 different velocity trends which are fast velocity trend (SG05 and SG07) and slow velocity trend (FUWN-28) corresponding to the pressure in wells. The overpressure zones can be identified as a slower velocity zone highlighted in red colour.

velocity volume can be used to estimate the magnitude of overpressure. The continuous RMS velocity cube comes from seismic processing. The RMS velocity volume was later converted to interval velocity by Dix's equation as shown in the equation below.

$$Vi = \sqrt{TiV^2rms_i - T_{i-1}V^2rms_{i-1})}$$

Furthermore, more than 25% of drilling non-productive time (NPT) is due to overpressure. In addition to decreasing the NPT, correct prediction of the pressure regime enables faster drilling, less formation invasion, and therefore improved reservoir integrity. Thus, accurate pore pressure prediction (PPP) is crucial. For pore pressure prediction, there are 2 methods: Eaton's and Miller's methods. Those two methods helps create 3D modelling. 3D model building generates a volume of pore pressure gradient (PPG) from seismic velocity volumes. In this study, 3D modelling by Eaton's method was selected because the factors calculated in Eaton's formula are empirically derived values from relevant well data and the interval velocity which are derived from seismic processing. Furthermore, this method first assumes that there is a depth section over which the pore pressure is hydrostatic and the sediments are normally compacted because of the systematic increase in effective stress with depth. Miller's method is a technique used to estimate pore pressure in 3D using the effects of the matrix and mudline velocities. Unloading is identified by the reduction in effective stress as the pore pressure increases rapidly under specific conditions. Also, the physical relationships built into the Miller's equation are: at zero effective stress, the velocity is simply the fluid velocity, and as the effective stress approaches infinity, the velocity approaches the matrix velocity which means by this method, the formula are not empirically derived values from relevant well data seismic volume like Eaton's method. Therefore, Eaton's method is suitable for applying and making 3D modelling.

Conventional pore pressure analysis is based on Terzaghi's and Biot's effective stress principle which states that total vertical stress (σv) (or overburden stress) is equal to the sum of the effective vertical stress (σe) and the formation pore pressure (PP) as follows:

$$\sigma v = \sigma e + PP$$

where;

σv = Total vertical stress

σe = Effective stress

PP = Formation pore pressure

Calculate total vertical stress (σv) from rock density which is overburden pressure (OBP) while Estimate vertical effective stress (σe) from seismic velocity using Eaton's method. As the result, pore pressure is then PP= σv- σe.

To calculate pore pressure prediction (PPP) volumes, an overburden pressure (OBP) volume is required. The overburden pressure (OBP) is the stress due to the weight of overlying rock. This is calculated through integration of density which is a transform of velocity volume (3D model building). The overburden pressure volume which is calculated by a transform of velocity volume is shown in Figure 9 and 10.

From the figure 9, it shows the RMS velocity volume which was converted to interval velocity (by Dix's equation) in depth volume in order to be used to calculate the overburden pressure (OBP) volume afterward. Figure 9 also shows 3D view of interval velocity in depth volume which was used to calculate OBP volume in figure 10. After an interval velocity in depth volume was generated, the OBP is calculated via the integration of a density volume which is a function of seismic velocity. Figure 10 shows the overburden pressure (OBP) volume which is the stress due to the weight of overlying rock. This is calculated by integration of density via a transform of velocity volume (3D model building mode).

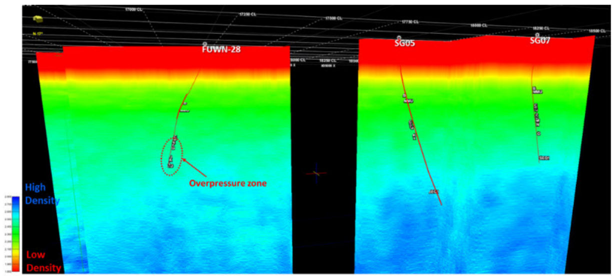

Figure 9 This is 3D view of interval velocity in depth volume. The RMS velocity volume was converted to Interval Velocity (by Dix's equation) in Depth volume in order to be used to calculate the OBP volume.

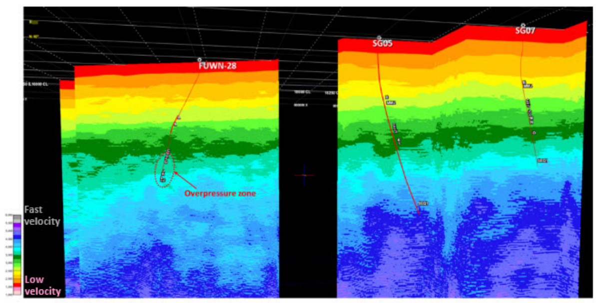

Figure 10 In 3D modelling, this is the overburden pressure (OBP) volume which is the stress due to the weight of overlying rock. The overburden pressure (OBP) volume is the stress due to the weight of overlying rock. This is calculated though integration of density via a transform of velocity volume (3D model building mode).

Eaton's method equations for PPP can be made from velocity data volumes (slowness derived from seismic interval velocity from a volume). Eaton's method predicts pore pressure from velocity, using equations shown below. This requires a normal compaction trend line (NCTL) and overburden pressure (OBP) derived from regional models.

From slowness (seismic velocity)

$$PP=OBP-(OBP-NP)*(DT_{NCTL}/DT)^{n}$$

Where;
PP = Pore Pressure (gradient)
OBP = Overburden pressure
NP = Normal pressure (hydrostatic gradient)
DT = Slowness from log
DT NCTL = Slowness of normal compaction trend line
n = exponent for DT

The Normal Compaction Trend Line (NCTL) can be derived from velocity NCTL which is the compaction trend for making pore pressure prediction from seismic interval velocity.

The result of pore pressure prediction by Eaton's method

Pore pressure = σv - σe

Where; σv = Overburden pressure

σe = Vertical effective stress derived from Eaton's equation

Isochronal Velocity Mapping

The seismic interval velocity cube shows an overall increasing interval velocity with depth. The well section comparison between normal and overpressure wells is shown in Figure 12. FUWN-28 (overpressure well) shows thicker time interval starting from 6,200 ft TVDss (around C marker) than time interval in SG05 and SG07 (normal pressure well). Thus, comparing the time thickness at the same interval, the time interval in the overpressure well is thicker due to slower velocity than in the normal pressure well.

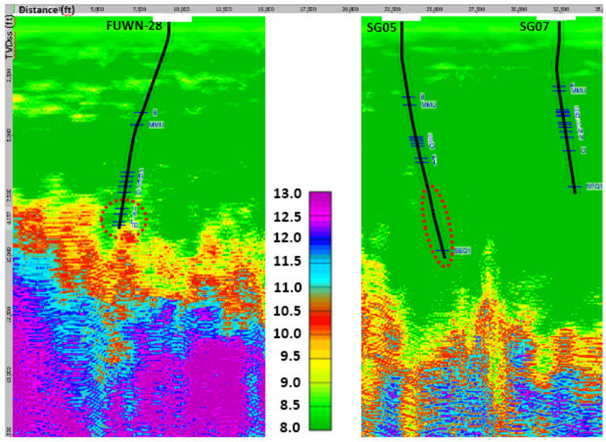

Figure 11 The result of pore pressure prediction by Eaton's method on the location of FUWN-28 well, SG05 and SG07 well is shown in Figure 19. It shows that Eaton's method cannot predict pore pressure precisely for the model because from the pressure report, the pressure recorded at FUWN-28 well TD is 12.3 ppg which should be shown in dark blue according to the colour bar scale but it is shown in yellow colour which indicates that the pressure there is around 9.5-10.0 ppg which is not correct. Also, from pressure report, the pressure recorded at SG05 at around 8,500 ft TVDss until 9,700 ft TVDss is around 8.8 ppg which should be shown in lemon green colour according to colour bar scale but it is shown in dark green colour which indicates that the pressure there is around 8.0-8.5 ppg which is not correct.

Isochronal velocities are mapped every 125 ft/ms starting from 3,000 to 4,000 ft/ms. The shallow section with the hydrostatic pressure (2,500 to 3,000 ft/ms) shows constant time thickness that corresponds to similar velocity in this interval. Although, this isochronal velocity mapping doesn't show the obvious evidence of different time intervals between overpressure area and normal pressure, there are still some changes that can be observed. This uncertainty might be because the velocity picking resolution is not high enough for observing the time interval and comparing between overpressure zone and normal pressure zone. However, it shows that the time thickness interval is larger when it is in the overpressure interval (3,000 to 4,500 ft/ms). The thicker intervals show pressure higher than 9.0-10.0 ppg (overpressure) starting at isochronal velocity 3,000 ft/ms. From velocity isochronal mapping (Figure 12), it shows variations in time thickness. The thicker interval corresponds to an area of overpressure. The conclusion is that the thicker time interval indicates slower velocity than thinner interval. Therefore, the thicker isochronal velocity represents the overpressure zone in the wells.

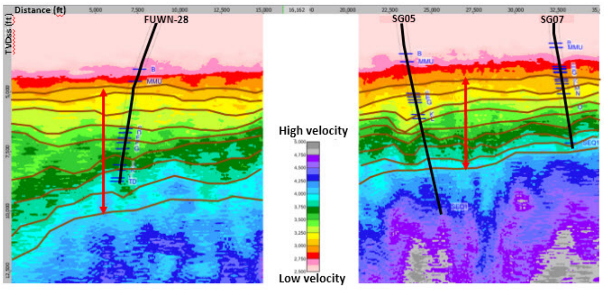

Figure 12 Velocity isochronal mapping from arbitrary line shows variations in time thickness. The thicker interval (red arrow) corresponds to an area of overpressure which starts from 6,200 ft TVDss related to C marker (Top Sequence 3).

5. Discussion and Conclusion

In this study, well log data and seismic data were used to identify overpressure. The first part of this study covered the overpressure studied based on well log data analysis. The last part of the study mentioned about the overpressure observed by seismic data.

There are many causes of overpressure; however, in this study area, the overpressure zone is probably caused by 1) Differential compaction which can be investigated by seismic and 2) Generation of hydrocarbons which cannot be investigated by seismic

1. Differential Compaction

At the appropriate temperature, hydrocarbon has been generated. In the basin center, the sediment is rapidly deposited more than the basin flank. It causes fluid expansion and the rock can no longer be compacted. This could cause differential compaction and eventually it causes overpressure. The overpressure caused by differential compaction can be detected by slow seismic velocity in seismic. As can be seen from velocity function plot resulted of well-tie-to-seismic. It shows that the overpressure well shows slower velocity than hydrostatic pressure well (figure 8). The onset of overpressure starts from C-D marker is related to Sequence 3 due to the data analysis from well log, well-tie-to-seismic and pressure profiles.

Also, from well log data, the deposition environment in Sequence 3 is interpreted as intertidal to fluvial environment which would consist of sand bodies sealed on all sides by impermeable shale as mentioned in regional work for depositional environment. Geologic overpressure in stratigraphic layers is caused by the inability of connate pore fluids to escape as the surrounding matrix compacts under the lithostatic pressure caused by overlying layers. Fluid escape may be impeded by sealing of the compacting rock by surrounding impermeable layers. Alternatively, the rate of burial of stratigraphic layer may be so great that the efflux of fluid is not sufficiently rapid to maintain hydrostatic pressure. This idea is supported by Morley and Racey, 2011. Moreover, the structural control and high subsidence rate caused rapid burial of sediments (Morley et al., 2011). The rapid burial rates resulted in shale sections becoming undercompacted as the fluids could not be expelled fast enough. Consequently, these shale intervals then became overpressure, especially in Sequence 3, which has a higher shale content than other sequences. The well logs show the evidence of higher organic shale content in Sequence 3 (C-K marker) compared to shale content from the sequence up (Sequence 4) and below it (Sequence 2). The average sand/shale ratio in Sequence 3 is higher than Sequence 2 and Sequence 4 (based on 3 well log study; FUWN-28, SG05 and SG07).

2. Generation of Hydrocarbons

Hydrocarbon generation associated with kerogen maturation in source rocks also causes of overpressure. As observed in Sequence 3, there are high organic-rich shales that can be good source rocks (Kamvan, 2013; Morley and Racey, 2011). The organic rich shale is mainly deposited in Sequence 3. Maturation studies show that with appropriate pressure and temperature conditions which is at depth around 6,000-9,000 ft TVDss with Ro = 0.65-1.30 (within hydrocarbon generation window), these organic-rich shales can generate hydrocarbons. The hydrocarbon can be expelled into the system resulting in higher pressure. From well log analysis, organic rich shale in Sequence 3 in FUWN-28 is more than organic rich shale in Sequence 3 in SG05 and SG07. The higher proportion of shale in FUWN-28 when subjected to the appropriate pressure and temperature conditions can generate hydrocarbons that causes overpressure. Whereas SG05 and SG07 are not overpressure because these two wells have lower amounts of organic rich shale (source rock) but they are also located too shallow for hydrocarbon generation. Therefore, these two wells do not show overpressure. This type of overpressure (Generation of Hydrocarbon) cannot be observed by seismic because the sediment has been compacted and then hydrocarbon has been generated. This causes overpressure in the pore space but it does not cause any expansion and the rock property has not been changed.

The stratigraphy of the sediment column plays an important role for pore pressure magnitude which means overpressure zones are horizon controlled not depth controlled. The FUWN-28 (overpressure well) is located towards into the basin and the thickness of Sequence 3 is thicker than Sequence 3 in SG05 well and SG07 well (normal pressure well) located at the basin flank. Sedimentation rate and subsidence rate at the basin flank is relatively slower than basin center which could lead to disequilibrium compaction and overpressure mechanism also. Moreover, the cause of overpressure may come from hydrocarbon generation. Organic rich shale is the source rock with increasing burial by later sediments and increase in temperature causes the kerogen within the rock to break down into hydrocarbons. The hydrocarbons generated from thermally mature source rock are first expelled, along with other pore fluids, due to the effects of internal source rock overpressuring caused by hydrocarbon generation as well as by compaction.

From the diagram (Figure 13) indicates that hydrocarbon generation window starts from 6,000 ft (approx.2,000m) to 9,000ft (approx.3,000m) (thermal gradient used) in Pattani Basin (modified from internal report; Chevron Texaco (Offshore) Thailand Ltd., 2001). The Sequence 3 in FUWN-28 has higher portion of organic rich shale than SG05 and SG07 and also FUWN-28 is in hydrocarbon generation window; whereas, Sequence 3 in well SG05 and SG07 is shallower than hydrocarbon generation window so it is too shallow to generate hydrocarbon. This evidence also supports the idea that the overpressure from FUWN-28 might be due to hydrocarbon generation as shown in Figure 13.

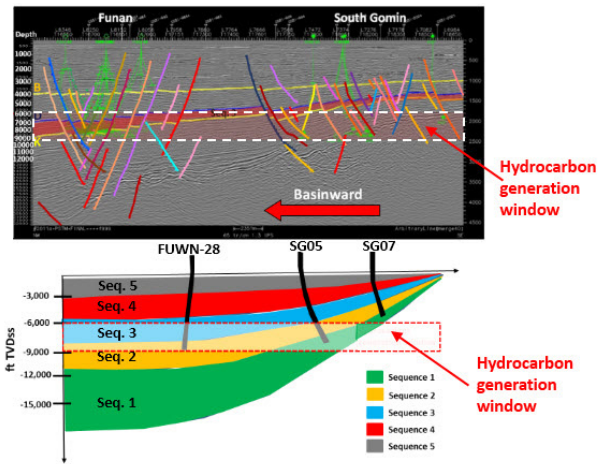

Figure 13 Overpressure from FUWN-28 can be due to 1) differential compaction and 2) hydrocarbon generation. From this diagram (modified from burial history diagram and maturation plot in Pattani Basin, Chevron internal report), the rate of burial of stratigraphic layer may be so great at the basinward (FUWN-28 location) and greater than basin flank (SG05 and SG07 location) that the efflux of fluid is not sufficiently rapid to maintain hydrostatic pressure and it causes overpressure. Another possibility is that it might be associated with hydrocarbon generation because Sequence 3, which has lots of organic rich shale, in FUWN-28 is within hydrocarbon generation window so hydrocarbon must be generated and causes overpressure. Sequence 3 in well SG05 and SG07 is shallower than hydrocarbon generation window. Thus, it doesn't show overpressure in SG05 and SG07.

Another part of this study is to identify overpressure by seismic data which are velocity isochronal mapping and Eaton's pore pressure prediction. Pore pressure prediction from seismic velocity volume by Eaton's method cannot predict pressure accurately as men tioned before because it is important to note that to calculate the magnitude of overpressure using seismic velocities may require a higher vertical resolution of the seismic velocity. The seismic velocity derived from stacking velocity is low frequency which depends on resolution of velocity picking.

In conclusion, the overpressure can be investigated by only well log but not on seismic as mentioned above. Both isochronal velocity mapping and Eaton's method for pore pressure prediction cannot predict overpressure in this area because overpressure that is caused by hydrocarbon generation cannot be directly detected by seismic. Also, possibly more work on detailed seismic picking velocity could help to refine this study.

6. References

Amonpantang, P., 2010, An overpressure investigation by sonic log and seismic data in Moragot Field, Gulf of Thailand: Master's thesis, Chulalongkorn University, Bangkok, 64 p.

Bell, D.W., 2002, Velocity estimation for pore pressure prediction, in Huffman A.R. and Bowers, G.L. editors, Pressure Regimes in Sedimentary Basins and Their Prediction, AAPG Memoir 76: 217-233.

Bowers, G.L. 1994, Pore Pressure estimation from velocity data: accounting for overpressure mechanisms besides undercompaction, IADC/SPE Drilling conference proceedings, p 515-530.

Dug insight 3.1 User Manual

Kananithikorn N., 2015, Seismic Characteristics of the overpressure area in southern Pattani Basin, Gulf of Thailand: Master's thesis, Chulalongkorn University, Bangkok, 43 p.

Morley C., A. Racey, 2011, Tertiary stratigraphy, in M. Ridd, A Barber, M. Crow, eds., The Geology of Thailand: London, The geological society, p. 223-271.

Morley C., P. Charusiri, I. Watkinson, 2011, Structural geology of Thailand during the Cenozoic, in M. Ridd, A Barber, M. Crow, eds., The Geology of Thailand: London, The geological society, p. 273-334.

Morley, C., R. Westaway, 2006. Subsidence in the super-deep Pattani and Malay Basins of Southeast Asia: a coupled model incorporating lower-crustal flow in response to post-rift sediment loading. Basin Research, v. 18, p. 51–84.